Applied Catalysis B: Environmental 96 (2010) 190–197

Contents lists available at ScienceDirect

Applied Catalysis B: Environmental

journal homepage: www.elsevier.com/locate/apcatb

Low temperature catalytic steam reforming of ethanol. 2. Preliminary kinetic investigation of Pt/CeO_2 catalysts

P. Ciambelli, V. Palma*, A. Ruggiero

Dipartimento di Ingegneria Chimica e Alimentare, Università degli Studi di Salerno, Via Ponte Don Melillo, 84084 Fisciano (SA), Italy

ARTICLE INFO

Article history:
Received 13 July 2009
Received in revised form 9 February 2010
Accepted 13 February 2010
Available online 19 February 2010

Keywords:
Fuel cell
Hydrogen production
Low temperature ethanol steam reforming
Pt/CeO_2 catalyst
Kinetics of ethanol reforming

ABSTRACT

Catalytic activity, selectivity and stability of a Pt/CeO_2 (5wt% Pt) catalyst were investigated in the low temperature ethanol steam reforming reaction for hydrogen production.

Experimental results showed that the catalyst is very active and selective, with negligible CO production and complete ethanol conversion already at 300 °C. The main promoted reactions are ethanol decomposition, ethanol steam reforming and CO water gas shift, and a preliminary kinetic investigation showed that the apparent reaction orders are 0.5 and 0 for ethanol and steam respectively, with an apparent activation energy of 18 kJ mol^{-1} evaluated in the range 300–450 °C.

Kinetic evaluations and temperature programmed desorption experiments suggest a surface reaction mechanism involving the following step: (i) ethanol dissociative adsorption on catalyst surface to form acetaldehyde intermediate, (ii) decarbonylation to produce mainly H_2, CH_4 and CO, and (iii) WGS reaction of CO adsorbed on Pt sites to produce H_2 and CO_2.

1. Introduction

One of the alternatives for clean energy generation is fuel cell technology. Polymer electrolyte membrane fuel cells (PEMFCs) powered by hydrogen are well-suited for both vehicles and distributed stationary facilities such as combined heat and power generation for houses and small-scale commercial applications. Since PEMFCs require a continuous supply of hydrogen, the use of an in situ catalytic fuel processor that will readily convert hydrocarbon fuels into hydrogen is a potentially feasible solution.

The criteria for the selection of the optimal hydrocarbon source for small-scale energy production include either a well-established distribution network, as in the case of natural gas, and/or a liquid fuel for easy storage and transportation, as in the case of gasoline. Although natural gas, gasoline and methanol are usually mentioned as the likely sources for hydrogen production, their use does not reduce reliance on fossil fuels or emission of pollutants.

Ethanol has recently received increased attention as a hydrogen source due to its crucial advantage of being available from renewable sources such as biomass, plants or waste materials from agriculture and forestry industries. Hydrogen production from bioethanol offers a nearly closed carbon loop since the carbon dioxide produced is consumed for biomass growth [1]. Moreover, ethanol is widely available, easily transportable, safe to handle and less toxic compared to methanol.

Steam reforming (SR) of ethanol is investigated in this context, since if compared with methane steam reforming, it has a very high efficiency for hydrogen production, but the reaction endothermicity:

$$CH_3CH_2OH + 3H_2O \rightleftarrows 6H_2 + 2CO_2, \quad \Delta H^{\circ}_{298\,K} = 173\,kJ\,mol^{-1} \quad (R1)$$

constitutes a major drawback, given that an external heat source is needed. The favored formation of CO at high temperatures is a further disadvantage, causing the necessity of hydrogen purification processes to reduce its content to concentrations tolerated by the PEMFCs.

Even though the overall steam reforming reaction looks straightforward, the reaction scheme is complicated by the presence of other reactions occurring in the system, depending mostly on reaction temperature and catalyst composition, and resulting in outlet streams containing hydrogen, carbon monoxide, carbon dioxide, methane, ethylene, acetaldehyde, etc. [2,3]. The most likely side reactions over Ni-based catalysts are ethanol SR with methane production, ethanol decomposition and methane SR:

$$CH_3CH_2OH + H_2O \rightleftarrows CH_4 + 2H_2 + CO_2 \quad (R2)$$

$$CH_3CH_2OH \rightleftarrows CH_4 + H_2 + CO \quad (R3)$$

$$CH_4 + H_2O \rightleftarrows CO + 3H_2 \quad (R4)$$

Methanation of carbon oxides may also be considered as a possibility. Comas et al. [3] studied ethanol SR over Ni/Al_2O_3 at 573–773 K

* Corresponding author. Tel.: +39 089964147; fax: +39 089964057.
E-mail address: vpalma@unisa.it (V. Palma).

0926-3373/$ – see front matter © 2010 Elsevier B.V. All rights reserved.
doi:10.1016/j.apcatb.2010.02.019

to propose a reaction scheme. Fatsikostas and Verykios [4] investigated the effect of using different supports for Ni catalysts and reported that carbon deposition is significantly reduced by impregnating γ-Al_2O_3 with La_2O_3. Sun et al. [5] suggested that ethanol steam reforming on Ni catalysts is first order with respect to ethanol and computed apparent activation energies between 1.87 and 16.88 kJ mol^{-1} depending on the type of catalyst support. Akande et al. [6] studied crude ethanol SR over Ni/Al_2O_3 and suggested a reaction order of 0.43 with respect to ethanol and activation energy of 4.41 kJ mol^{-1}. More recently, also in the case of noble metals based catalysts, different studies showed that the support plays an important role to determine the catalytic performances in terms of activity, selectivity and stability of the final catalyst in both methane [7] and ethanol partial oxidation and steam reforming reactions, [8,9], favoring different reaction pathways depending on the support nature. In particular, it is reported that in the case of $Pt/CeZrO_2$ [10] ethanol adsorbs as ethoxy species, which may follow one of two distinct pathways: (i) decomposition and production of CO, CH_4, and H_2 or (ii) dehydrogenation to acetaldehyde and acetyl species. The dehydrogenated species may undergo oxidation to acetate species, also promoted by the addition of water to the feed. Water also facilitated the decomposition of acetaldehyde and acetate reactions, resulting in the formation of methane, CO, and carbonate. A deactivation mechanism for the catalytic ethanol decomposition and steam reforming reactions at 773 K on $Pt/CeZrO_2$ catalyst was also proposed by de Lima et al. [11], based on the loss of the Pt-support synergy, leading to a buildup of carbonaceous residue on the catalyst surface.

Finally, although the catalytic ethanol SR reaction has recently received more attention, extended parametric and kinetic studies are scarce [12], especially at low temperature. Intrinsic kinetics of ethanol SR studied over Ru/Al_2O_3 using excess water, on the other hand, showed that ethanol conversion was directly proportional to ethanol partial pressure and independent of steam partial pressure with apparent activation energy of 96 kJ mol^{-1} [13].

The present work focuses on ethanol SR over Pt/CeO_2 catalyst, which is a successful catalyst for this reaction in the low temperature range, as from the first part of this work [14]. A parametric study was carried out to reveal the effects of space–time, water to ethanol molar ratio and temperature on ethanol conversion and hydrogen formation. Being the rate law determined in kinetic regime closely related to the reaction mechanism, specific experimental tests have been conducted in order to determine the reaction order for the reactants and propose a power-function rate expression for ethanol conversion. Moreover, ethanol and ethanol–water adsorption–desorption experiments were also performed in order to further investigate the reaction mechanism.

2. Experimental

2.1. Catalysts preparation and characterization

A series of Pt/CeO_2 catalysts (Pt loading 1–5 wt%) were prepared by wet impregnation of CeO_2 (46 m^2/g, Aldrich), drying and calcining, as reported in Part I [14], where values of BET specific surface and the nominal metal content are also reported. In that study we found that the catalyst containing 5 wt% Pt (5-Pt/CeO_2), give the highest hydrogen yield with the lowest CO formation, and was more stable with respect to lower Pt load formulations.

TPR characterization test showed the presence on CeO_2 surface of highly dispersed PtOx species and the presence of direct Pt–O–Ce bonding, where the strong interaction of PtOx with the CeO_2 support retards the reduction of the supported PtOx phase to metallic Pt [15]. At higher Pt load, the effectiveness of the PtOx phase dispersion decreases, and the lower extent of the Pt–O–Ce bonding results in a lower reduction temperature, with the formation of metallic Pt at temperature lower than 90 °C.

2.2. Catalytic tests of ethanol steam reforming

Catalytic testing of ethanol steam reforming (ESR) was carried out with the laboratory apparatus reported in Part I [14]. The performance of catalysts was evaluated with a fixed-bed quartz reactor (18 mm i.d.) placed in a three heating zones electric furnace equipped with three PID temperature controllers. A K type thermocouple was placed at the middle of the catalyst bed to monitor the reactor temperature. Catalyst samples were tested at atmospheric pressure by changing reaction temperature, contact time and steam to ethanol molar ratio. Before each ESR test the catalysts were reduced in situ with a 5 vol.% hydrogen in nitrogen gas stream heating to 600 °C at 20 °C/min and keeping that temperature during 1 h. The reactor was operated isothermally in plug-flow mode at steady state conditions. Ethanol and water were sent to the reactor after nitrogen streams saturation in two temperature controlled saturators, mixing, and further dilution with nitrogen. The reactor outlet gas was monitored with an on line FT-IR multigas analyzer (Nicolet Antaris IGS, Thermo Electron S.p.A.). The spectrophotometer is equipped with 2- and 10-m fixed path length heated gas cell operating at temperatures up to 185 °C, and an MCT-A detector cooled with liquid nitrogen. Dedicated analysis software allows to follow simultaneously up to 100 different species in the gas phase. The spectra were collected with the 2-m gas cell maintained at 150 °C. Cell temperature and pressure were monitored and used to correct gas concentration values. The FT-IR data were acquired at 0.5 cm^{-1} resolution. H_2 concentration in the product gas stream was analyzed by a thermoconductivity analyzer (ABB, CALDOS 27).

The effect of internal and external diffusional resistance on the catalytic performances was evaluated through preliminary runs at 300 and 450 °C with catalyst particle size ranging from 40 to 710 μm and gas flow rate from 250 to 2000 (stp) cm^3/min. Kinetic data were collected by varying contact time, temperature and steam to ethanol molar ratio. Specifically, reaction temperature from 300 to 450 °C, ethanol partial pressure between 0.005 and 0.01, water partial pressure between 0.005 and 0.03 atm, water/ethanol molar ratio in the range 1.5–6.0, and space–time from 0.1 to 17 mg min μmol^{-1}, were investigated. In kinetic experiments 50 mg of fresh sample was used in order to assure differential reactor mode.

2.3. Temperature programmed desorption (TPD) of ethanol

Ethanol TPD experiments were carried out in the same apparatus described for SR catalytic tests. The adsorption of ethanol was carried out at room temperature by feeding 1 vol.% ethanol in N_2 gas mixture. After adsorption saturation the gas mixture was switched to 1000 (stp) cm^3/min pure nitrogen flow and the catalyst sample was heated at 10 °C/min up to 600 °C. TPD tests in the presence of 1 vol.% water in N_2 were also carried out.

3. Results

3.1. Effect of metal loading on catalytic properties

The effect of Pt loading on ethanol steam reforming was first investigated under isothermal conditions at 300 °C, and the results are reported in Table 1 in comparison with the thermodynamic equilibrium values. Ethanol conversion (X), H_2 yield (Y) and prod-

Table 1
Ethanol conversion (X), hydrogen yield (Y) and products selectivity (S) for Pt/CeO_2 catalysts after 3 h of time on stream.

Catalyst	X_{EtOH} (%)	Y_{H_2} (%)	S_{CH_4} (%)	S_{CO} (%)	S_{CO_2} (%)	S_{H_2} (%)	$S_{C_3H_6O}$ (%)	S_C (%)
CeO_2	6	<1	10	<1	10	4	0	–
1-Pt/CeO_2	100	29	32	21	26	29	16	–
3-Pt/CeO_2	100	39	44	2	56	39	1	–
5-Pt/CeO_2	100	38	40	0	59	38	–	–
Equilibrium	100	18	56	0	33	18	0	10

Experimental conditions: T = 300 °C; EtOH = 0.5 vol.%; EtOH:H_2O:N_2 = 0.5:1.5:98; total gas flow rate = 1000 (stp) cm^3/min; GHSV = 15,000 h^{-1}.

ucts selectivity (S) are defined as in Eqs. (1)–(8):

$$X_{C_2H_5OH} = \frac{n^{in}_{C_2H_5OH} - n^{out}_{C_2H_5OH}}{n^{in}_{C_2H_5OH}} \quad (1)$$

$$S_{H_2} = \frac{n_{H_2}/6}{n^{in}_{C_2H_5OH} - n^{out}_{C_2H_5OH}} \quad (2)$$

$$S_{CH_4} = \frac{n_{CH_4}/2}{n^{in}_{C_2H_5OH} - n^{out}_{C_2H_5OH}} \quad (3)$$

$$S_{CO} = \frac{n_{CO}/2}{n^{in}_{C_2H_5OH} - n^{out}_{C_2H_5OH}} \quad (4)$$

$$S_{CO_2} = \frac{n_{CO_2}/2}{n^{in}_{C_2H_5OH} - n^{out}_{C_2H_5OH}} \quad (5)$$

$$S_{C_3H_6O} = \frac{3n_{C_3H_6O}}{2(n^{in}_{C_2H_5OH} - n^{out}_{C_2H_5OH})} \quad (6)$$

$$S_C = \frac{n_C/2}{n^{in}_{C_2H_5OH} - n^{out}_{C_2H_5OH}} \quad (7)$$

$$Y_{H_2} = \frac{n_{H_2}/6}{n^{in}_{C_2H_5OH}} \quad (8)$$

While at the experimental conditions employed CeO_2 alone showed a very low activity and stability in ethanol conversion (about 12% after 1 h and 6% after 3 h TOS), total conversion of ethanol was obtained for all Pt/CeO_2 catalysts. The product distribution is affected by metal loading, 3-Pt/CeO_2 showing the highest selectivity to H_2 and CH_4. Selectivity to CO_2 monotonically increases with Pt content, while selectivity to CO and to acetone decreases to 0 on 5-Pt/CeO_2.

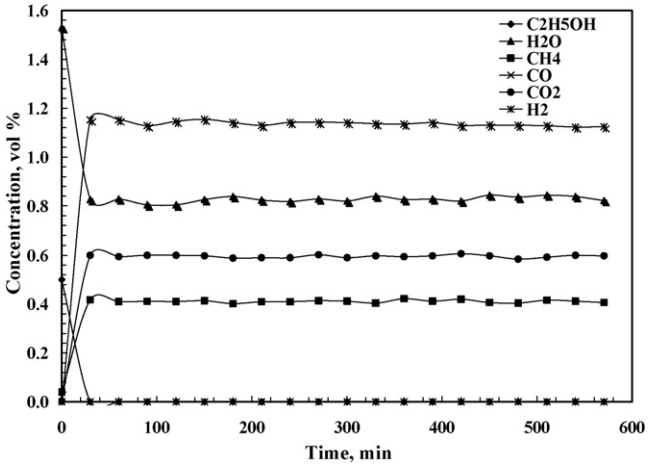

Fig. 1. Stability test of 5-Pt/CeO_2 catalyst. Experimental conditions: T = 300 °C; EtOH = 0.5 vol.%; EtOH:H_2O:N_2 = 0.5:1.5:98; total gas flow rate = 1000 (stp) cm^3/min; GHSV = 15,000 h^{-1}.

In Fig. 1 the results of a 10 h stability test of 5-Pt/CeO_2 are reported. Taking into account these results together with the activity and selectivity performances (see also Part I [14]) we selected this catalyst for a preliminary kinetic investigation.

3.2. Influence of operating conditions on ESR kinetics

3.2.1. Effect of space–time

The effect of space–time on products distribution, investigated at constant temperature of 300 °C and water to ethanol molar ratio = 3, is shown in Fig. 2. From the data relevant to the formation of H_2, CO and CH_4 at very low space–time, it turns out evident that only these three are primary products of ethanol conversion and no appreciable amount of CO_2 is formed. On the other hand at very low space–time also the water conversion is close to zero. At higher space–time the CO curve shows a maximum, the water mole fraction decreases, and the CO_2 formation becomes evident. These behaviors suggest that CO_2 seems to be formed by consecutive reactions. The latter conclusion is also confirmed by the quantitative accordance between the amount of water consumed and CO_2 formed, indicating that the water gas shift reaction takes place in the reactor at higher space–time values. The selectivity to H_2 and CH_4 increases with the space–time. We did not find any change of products distribution for much longer space–time (up to 17 mg min μmol^{-1}).

3.2.2. Effect of reaction temperature

The effect of reaction temperature on the products distribution was investigated at 300, 400 and 450 °C, varying the space–time from 0.1 to 17 mg min μmol^{-1} at constant water to ethanol molar ratio of 3. Ethanol and water conversions as function of space–time and temperature are reported in Fig. 3.

At fixed temperature both ethanol and water conversions increase by increasing space–time from 0.1 to 3 mg mol s^{-1}; no significant variation is observed for further increase to 17 mg min μmol^{-1}. While complete ethanol conversion is achieved

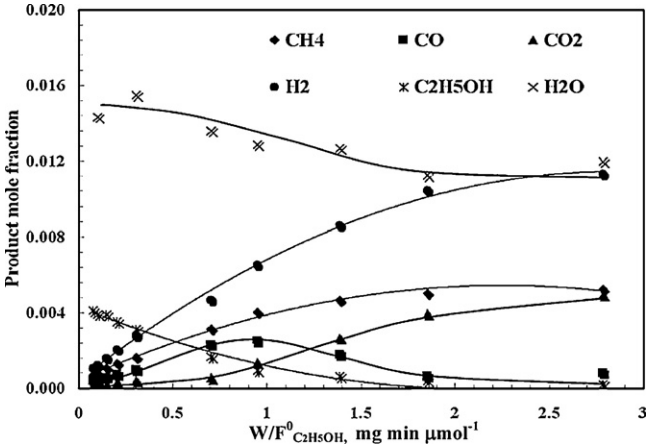

Fig. 2. Products distribution of ESR on 5-Pt/CeO_2 catalyst vs space–time. T = 300 °C, P = 1 atm, P_{EtOH} = 0.005 atm, H_2O:EtOH = 3:1 (mol:mol).

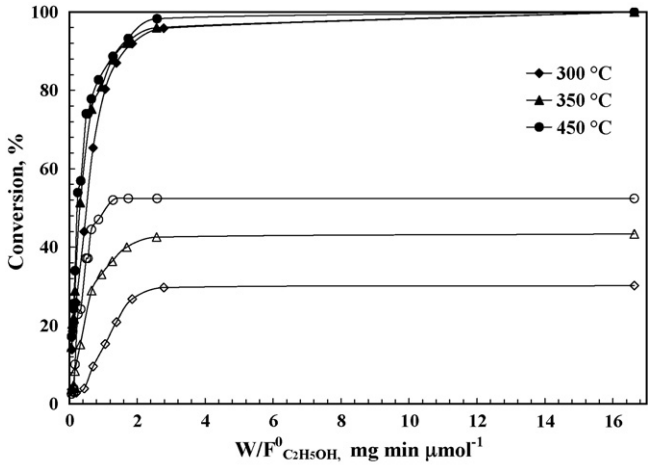

Fig. 3. Ethanol (full symbols) and water (void symbols) conversion vs space–time on 5-Pt/CeO_2 catalyst at different temperatures. P = 1 atm, P_{EtOH} = 0.005 atm, H_2O:EtOH = 3:1 (mol:mol) and total gas flow rate = 1000 (stp) cm^3/min.

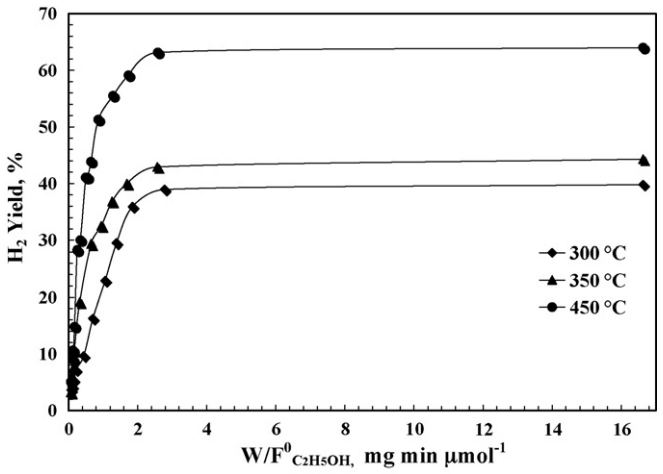

Fig. 4. Hydrogen yield vs space–time on 5-Pt/CeO_2 catalyst at different temperatures. P = 1 atm, P_{EtOH} = 0.005 atm, H_2O:EtOH = 3:1 (mol:mol) and total gas flow rate = 1000 (stp) cm^3/min.

at all temperatures, the water conversion is always lower, even if it increases by increasing the temperature from 300 to 450 °C at all space–times. A quite similar behavior is found for hydrogen yield, reported as function of space–time at 300, 350 and 450 °C in Fig. 4.

By increasing the temperature from 300 to 350 °C the hydrogen yield weakly increases at all space–times, while it is strongly enhanced at 450 °C.

The effect of space–time and reaction temperature on products selectivity is reported in Fig. 5.

At $W/F^0_{C_2H_5OH}$ higher than 4 mg min μmol^{-1}, the reaction products are almost exclusively H_2, CO_2 and CH_4. Therefore, it seems that ethanol decomposition (reaction (R3)), ethanol steam reforming (reaction (R1)), and water gas shift (reaction (R5)) are mainly promoted on this catalyst.

$$CO + H_2O \rightleftarrows H_2 + CO_2 \quad (R5)$$

Moreover, the slope change in the CO, CO_2 and H_2 selectivity curves reported in Fig. 5, gives evidence of the occurrence of WGS as consecutive reaction. In particular, this occurrence is more evident at lower reaction temperature, likely due to the exothermicity of WGS reaction.

Finally, the change in methane and H_2 selectivity at higher temperature is likely related to the concurrence of additional reactions such as

$$CH_4 + H_2O \rightleftarrows 3H_2 + CO \quad (R6)$$

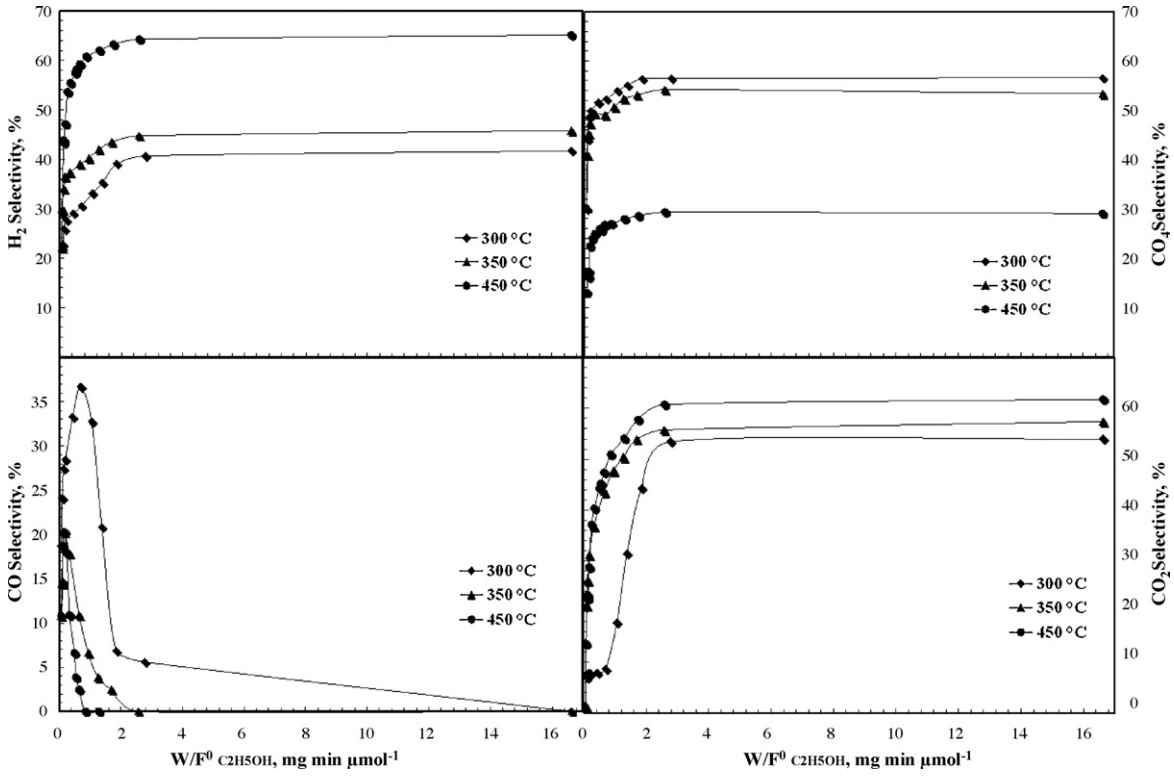

Fig. 5. Selectivity to H_2, CH_4, CO and CO_2 on 5-Pt/CeO_2 vs space–time at different temperatures. P = 1 atm, P_{EtOH} = 0.005 atm, H_2O:EtOH = 3:1 (mol:mol) and total gas flow rate = 1000 (stp) cm^3/min.

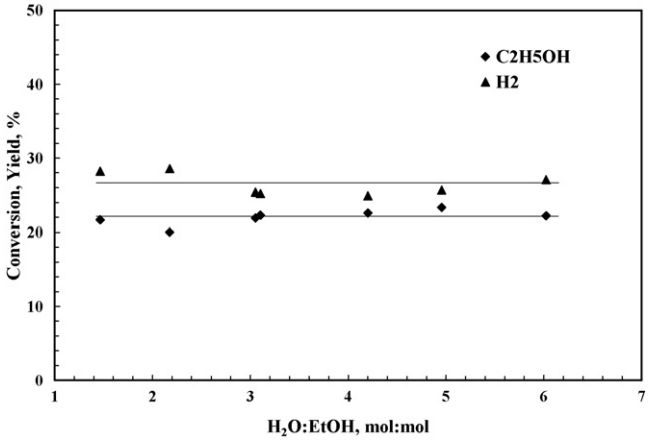

Fig. 6. Ethanol conversion and hydrogen yield vs water to ethanol molar ratio on 5-Pt/CeO_2 catalyst. T = 300 °C, P = 1 atm, P_{EtOH} = 0.005 atm and total gas flow rate = 1000 (stp) cm^3/min.

This suggestion is also supported by the water conversion trend exhibiting a further slope change at T > 300 °C (Fig. 3).

Finally, trace amounts of acetone (about 10 ppm) were formed up to 350 °C, likely produced by the reaction of acetaldehyde with adsorbed methyl groups [16], or by reaction of two ethanol molecules adsorbed [24].

3.2.3. Effect of water to ethanol molar ratio

The effect of water/ethanol molar ratio (W/E) on the steam reforming performance of 5-Pt/CeO_2 catalyst at 300 °C is shown in Fig. 6. It is evident that both ethanol conversion and hydrogen yield are almost not dependent of W/E in the investigated range (W/E = 1–6).

4. Preliminary kinetic investigation of ethanol steam reforming

4.1. Evaluation of internal and external diffusional resistance

Preliminary ESR runs were carried out with different catalyst particle size from 40 to 710 μm at 300 and 450 °C. Fig. 7 shows that the ethanol conversion is almost constant for a particle size diameter ranging from 50 to about 400 μm, indicating that the reaction rate is not limited by internal diffusion resistance in this range of diameter values. Therefore, we selected a particle diameter range of 180–355 μm for the kinetic runs.

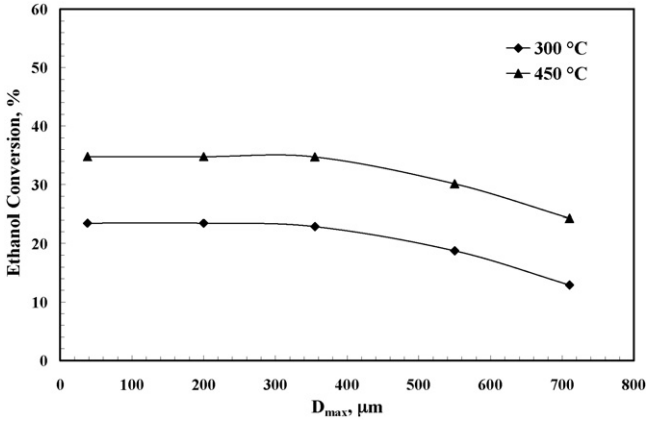

Fig. 7. Ethanol conversion on 5-Pt/CeO_2 catalyst as function of particle size at 300 and 450 °C. P = 1 atm, P_{EtOH} = 0.005 atm, H_2O:EtOH = 3:1 (mol:mol), and total gas flow rate = 1000 (stp) cm^3/min.

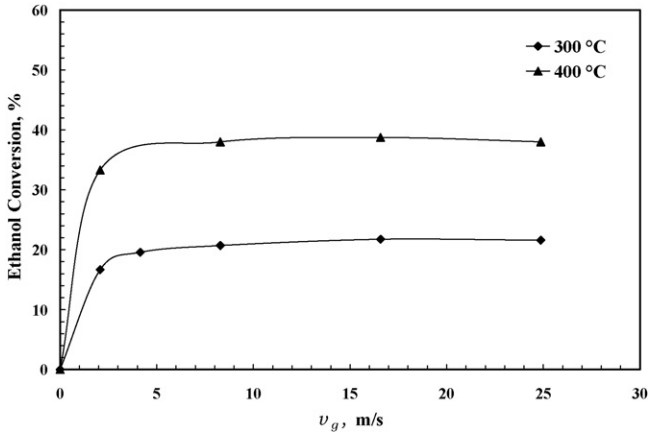

Fig. 8. Ethanol conversion on 5-Pt/CeO_2 catalyst as function of gas velocity at 300 and 400 °C. P = 1 atm, P_{EtOH} = 0.005 atm, H_2O:EtOH = 3:1 (mol:mol), and W/F^0_{EtOH} = 0.14 mg min μmol^{-1}.

The effect of gas velocity on ethanol conversion was also evaluated varying the volumetric flow rate from 250 to 3000 (stp) cm^3/min at 300 and 400 °C (Fig. 8).

Since the ethanol conversion is almost constant in the gas velocity range 5–25 m/s for the temperatures examined, a volumetric flow rate higher than 1000 (stp) cm^3/min has been used for all the kinetic runs in order to attain a gas velocity of about 10 m/s.

4.2. Evaluation of kinetic parameters

Kinetic runs were carried out by varying the partial pressure of one reactant, keeping constant the other operating conditions, and measuring the rate of ethanol conversion. Nitrogen was used as diluent. Details of experimental conditions are presented in Table 2. The very large values of GHSV investigated (about 2×10^6 h^{-1}) resulted in ethanol conversion lower than 20%, i.e. in differential reactor operation.

The experiments followed the Ostwald isolation method; in the first series ethanol partial pressure was kept constant at 0.5 vol.%, while water to ethanol molar ratio was varied from 1 to 6. The results showed that the ethanol consumption rate remained constant as a function of the steam partial pressure in the range investigated, suggesting a zero apparent reaction order with respect to steam (Fig. 9). In the second series of experiments water partial pressure was kept constant at 1.5 vol.%, while ethanol concentration was varied from 0.1 to 1 vol.%. In Fig. 10 the ethanol reaction rate is plotted against the square root of ethanol partial pressure at constant water partial pressure of 0.015 atm, suggesting a 0.5 apparent reaction order with respect to ethanol.

In the third series of experiments ethanol partial pressure and water to ethanol molar ratio were kept constant at 0.5 vol.% and 3, respectively, while the temperature was varied from 300 to 450 °C in order to evaluate the apparent activation energy (E_A) and the pre-

Table 2
Experimental conditions for kinetic parameters evaluation.

Description	Values
Catalyst weight (g)	0.05
Reaction temperature (°C)	300
C_2H_5OH/N_2 flow rate ((stp) cm^3/min)	4–45
H_2O/N_2 flow rate ((stp) cm^3/min)	50–300
N_2 flow rate ((stp) cm^3/min)	Balance to 1000
C_2H_5OH inlet partial pressure (atm)	0.001–0.01
H_2O inlet partial pressure (atm)	0.005–0.03
Total pressure (atm)	1
Gas hourly space velocity (h^{-1})	1,936,800

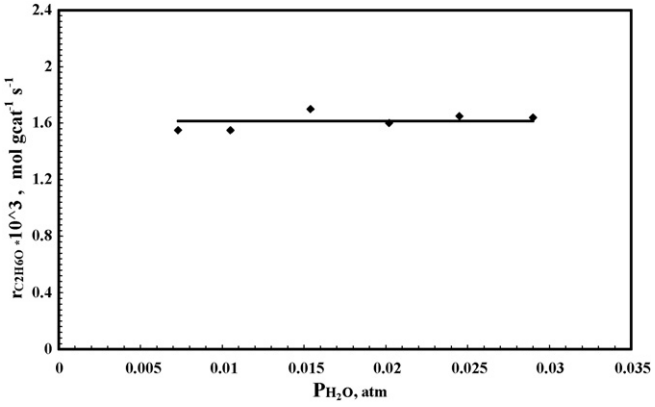

Fig. 9. Reaction rate of ethanol on 5-Pt/CeO_2 versus water partial pressure (P_{EtOH} = 0.05 atm, T = 300 °C, and GHSV = 1,936,800 h^{-1}).

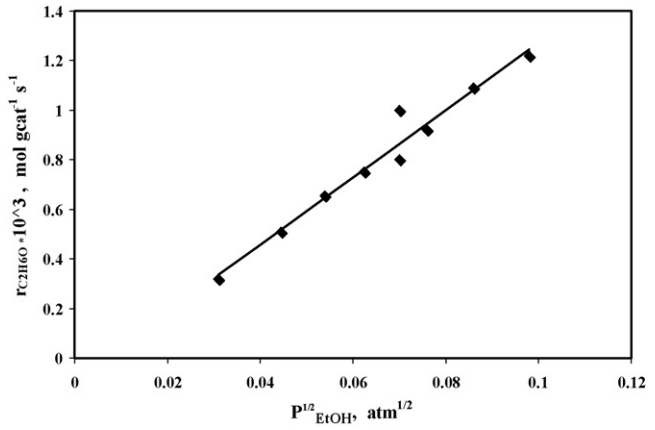

Fig. 10. Reaction rate of ethanol on 5-Pt/CeO_2 versus ethanol partial pressure (P_{H_2O} = 0.015 atm, T = 300 °C, and GHSV = 1,936,800 h^{-1}).

exponential factor (k_0). The obtained Arrhenius plot is reported in Fig. 11.

4.3. Power law modelling of the kinetic data

The general form of the empirical power-function rate expression for ethanol conversion was assumed as (Eq. (9)):

$$-r_{C_2H_5OH} = \left[k_0 \exp\left(-\frac{E_A}{RT}\right)\right](P_{C_2H_5OH})^{\alpha}(P_{H_2O})^{\beta} \quad (9)$$

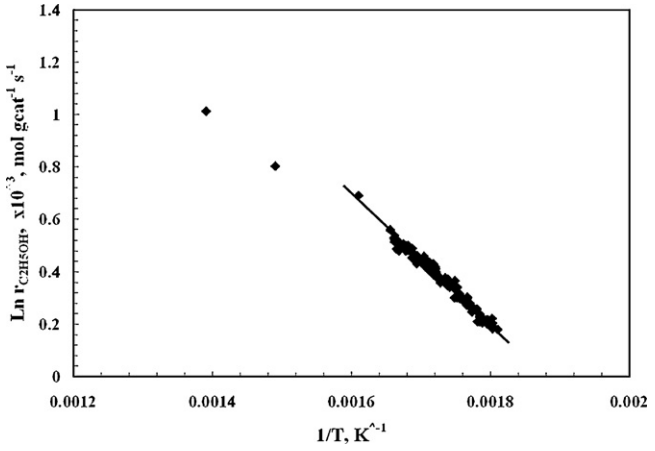

Fig. 11. Arrhenius plot of ethanol reaction rate on 5-Pt/CeO_2.

Table 3
Kinetic parameters of ethanol reaction rate on 5-Pt/CeO_2.

Parameters	Units	Estimates
K_0	mol g_{cat}^{-1} s^{-1} $atm^{-0.5}$	0.088 ± 0.02
E_A	kJ mol^{-1}	18.4 ± 2.1
α		0.5 ± 0.05
β		0 ± 0.015

The evaluation of the rate parameters α, β, k_0 and E_A involves the calculation of the reaction rates from ethanol conversion versus residence time data. A microreactor was used to gather the experimental data and the conversion equation for plug-flow differential reactor was applied for data analysis in the form (Eq. (10)):

$$\frac{dX}{dW/F_{A0}} = -r_A \quad (10)$$

where slopes $dX/(dW/F_{A0})$ were taken at various values of the X vs W/F_{A0} curves within the range of the experimental conditions investigated in order to obtain experimental rate data.

The values of the power law model parameters were estimated by a non linear regression procedure involving the minimization of the sum of the squared differences of the measured and the calculated reaction rate having the form (Eq. (11)):

$$\sigma^2 = \frac{\sum_{i=1}^{N}(r_{im} - r_{ic})^2}{N - P - 1} \quad (11)$$

where N is the number of the runs, P is the number of parameters to be determined, r_{im} is the measured reaction rate of the run i and r_{ic} is the calculated reaction rate of the run i.

The results of calculations, performed with the aid of SOLVER, a built-in subroutine provided by Microsoft Excel, are collected in Table 3.

The estimated reaction orders show that the rate of ethanol steam reforming is directly proportional to the square root of the partial pressure of ethanol and is not inhibited by the steam partial pressure. This result would probably indicate the occurrence of a reaction mechanism where dissociative adsorption of ethanol on the catalyst active sites is involved in the rate determining step, in agreement with the mechanism recently proposed by Jacobs et al. [17].

The dependence of ethanol steam reforming rates on steam partial pressure has not been sufficiently addressed in the literature. The high discrepancy and the low values of the activation energy and the different operating conditions of kinetic investigations reported in the literature [5,6,19,18] make difficult a comparison. However, the results obtained in this work indicate that the catalytic steam reforming of ethanol over Pt/CeO_2 catalyst does not involve water in the rate determining step. Moreover, no mass transfer process (external or internal) influenced the rate of reaction.

4.4. Temperature programmed desorption of ethanol

In order to better elucidate the reaction mechanism a TPD investigation was carried out. The ethanol TPD profiles from 5-Pt/CeO_2, before and after Pt reduction, and after 1 vol.% adsorption of ethanol at room temperature (Fig. 12) show that major desorbed products are CH_4, CO, CO_2, H_2, and acetaldehyde. At low temperatures the catalyst exhibited a wide intense H_2 desorption peak (maximum temperature of 185 °C). A smaller desorption peak of CH_4 (maximum temperature of 270 °C) and a large and tailed peak of CO_2 (T_{max} = 250 °C) were also detected, while no CO desorption was measured. The formation of H_2, CH_4, and CO in the low-temperature region during TPD of ethanol from Al_2O_3- and CeO_2-supported metals has been reported in [19–23]. Acetaldehyde also desorbs

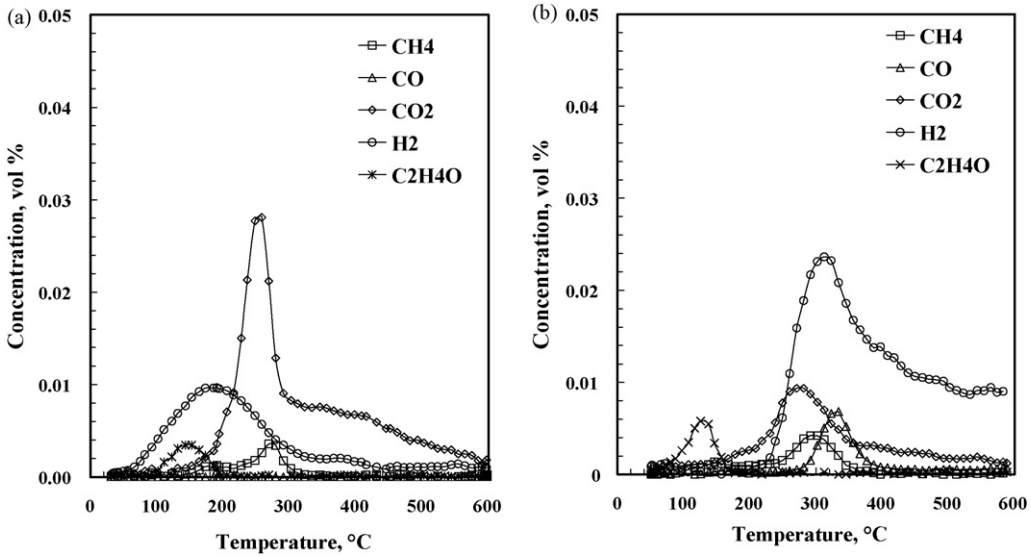

Fig. 12. Ethanol TPD profile after adsorption at room temperature on unreduced (a) and reduced (b) 5-Pt/CeO_2 catalyst (ethanol adsorption carried out at P_{EtOH} = 0.01 atm).

from the surface of calcined catalyst at low temperature, reaching a maximum at 147 °C (Fig. 12a). Erdohelyi et al. [24] reported the formation of acetaldehyde at around 230 °C over CeO_2- and Al_2O_3-supported noble metal catalysts and associated this formation to ethanol dehydrogenation and dehydration, respectively.

At higher temperatures (250–270 °C) two peaks of CO_2 and CH_4 are observed along with H_2 desorption. Previous studies [19,21,22] report the formation of CO and CH_4 above 230 °C during TPD of ethanol from CeO_2- and Al_2O_3-supported catalysts, and assign their formation to the decomposition of carbon species (i.e., acetaldehyde and acetate species) previously formed.

After catalyst reduction (Fig. 12b) only the desorption of acetaldehyde was detected in the low temperature range (131 °C), while no ethanol decomposition was observed in the range 100–200 °C. In the higher temperature range, from 200 to 400 °C, the desorption of CO_2, H_2, CH_4 and CO was detected as peaks at 275, 317, 301 and 333 °C, respectively. H_2 and CO_2 desorbed until the end of the test.

The main difference in the TPD results obtained for Pt/CeO_2 before and after reduction is that the reduced catalyst exhibits desorption of CO and larger desorption of CH_4 at high temperatures. These results suggest that the catalyst reduction promotes also the decomposition of carbon species previously formed (acetaldehyde and acetate species). In addition, the dissociation of CO_2 on oxygen vacancies of the support is favored. According to the literature, O_2 can replenish the oxygen vacancies of the CeO_2 support, releasing CO as a product [25].

The results of TPD from the reduced catalyst, carried out in the presence of water, are reported in Fig. 13. When water was added to nitrogen stream larger amounts of acetaldehyde were detected at 105 °C and a larger amount of hydrogen desorbed in all temperature range with two peaks at 180 and 275 °C. At 180 °C the desorption of CO_2, CH_4 and trace of CO was also detected. In the range 200–300 °C, CO_2 and CH_4 desorption was observed with peaks at 275 and 268 °C, respectively. In the same range of temperature a marked consumption of water, shown by two peaks at 240 and 400 °C, was detected. It must be remarked that in the presence of water a sensible increase in the H_2 and CO_2 desorption and a very lower formation of CO were detected with respect to the same test performed without water (Fig. 12b). Moreover, in the temperature range 180–500 °C, the water consumption profile is in good agreement with the H_2 and CO_2 desorption profiles, indicating that the

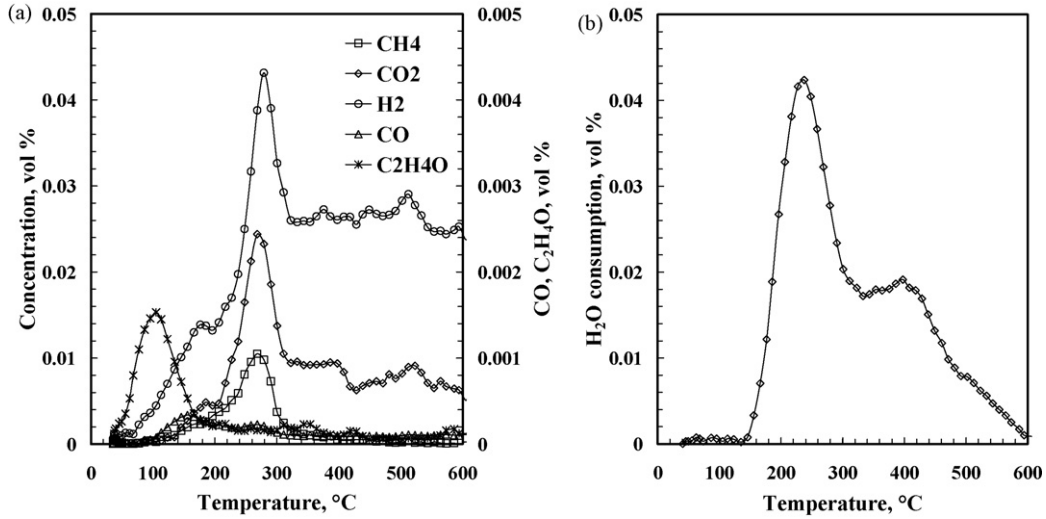

Fig. 13. TPD profile in the presence of water (a) and water consumption (b) after ethanol adsorption at room temperature on 5-Pt/CeO_2 catalyst after reduction step.

water vapor plays an important role by enhancing the decomposition of the intermediate carbonaceous compounds formed onto the catalyst surface during the adsorption step. Also in this case the experimental results suggest that the main role of water seems to be to promote the WGS reaction to produce more H_2 and CO_2, by consuming CO.

4.5. Reaction mechanism

The catalytic tests carried out at different contact times revealed that ESR proceeds through ethanol decomposition and water gas shift reaction. Kinetic evaluations suggest a surface reaction mechanism comprising the ethanol dissociative adsorption on the catalyst surface not involving water in the rate limiting step. Moreover, TPD experiments suggest that the reaction seems to proceed through acetaldehyde formation. On the other hand, it was experimentally demonstrated that ethanol adsorbs molecularly at 100 K on Pt [26,27]. Vesselli et al. [28] studied ethanol decomposition on Pt(1 1 1), concluding that ethanol adsorbs dissociatively on Pt surface through a metastable intermediate, identified as acetyl. Subsequently, acetyl dehydrogenates to ketenyl which undergoes decarbonylation to form CO and CH or CH_3. In the same work they evaluated the adsorption energy and the reaction barriers of the possible reaction intermediates for ethanol decomposition on Pt(1 1 1), identifying ketenyl (CHCO) as the intermediate with the lowest C–C cleavage barrier. It is worthwhile that if one considers the ethanol adsorption through acetaldehyde intermediate as the rate determining step, the value of the apparent activation energy calculated from Vesselli et al. [28] is in very good agreement with that obtained from our experiments.

Therefore, we propose that the reaction mechanism for the steam reforming of ethanol on Pt/CeO_2 catalysts comprises: (i) ethanol adsorption, (ii) an acetaldehyde intermediate formation, (iii) intermediate C–C bond rupture to produce H_2, carbon oxides, and CH_4 (iv) CO WGS conversion to CO_2.

In this view, the role of water is not in the direct mechanism of ESR, but, as shown by TPD, it is of primary importance in the catalyst regeneration stage promoting the decomposition reaction of carbon compounds previously formed.

5. Conclusions

Ethanol steam reforming over Pt/CeO_2 with 5 wt% metal loading was studied at 300–450 °C. The catalyst is very active and selective for the production of H_2 at low temperature, allowing total ethanol conversion with zero selectivity to CO.

We have found that the main reactions involved in the ethanol conversion are ethanol decomposition, ethanol steam reforming and water gas shift, and that 300 °C is the optimum reaction temperature in order to steam reform ethanol on 5-Pt/CeO_2 for hydrogen production and/or to pre-reform ethanol to obtain H_2 and CH_4 rich stream.

An empirical power-function rate equation has been proposed and apparent reaction orders of 0.5 and 0 have been calculated for ethanol and steam, respectively. The apparent activation energy and the pre-exponential factor evaluated in the range 300–450 °C are 18 kJ mol^{-1} and 0.088 mol g_{cat}^{-1} s^{-1} $atm^{-0.5}$, respectively.

Kinetic evaluations and temperature programmed desorption experiments suggest a surface reaction mechanism involving the following step: (i) ethanol dissociative adsorption on catalyst surface to form acetaldehyde intermediate, (ii) decarbonylation to produce mainly H_2, CH_4 and CO, and (iii) WGS reaction of CO adsorbed on Pt sites to produce H_2 and CO_2.

References

[1] D.K. Liguras, K. Goundani, X.E. Verykios, J. Power Sources 130 (2004) 30.
[2] F. Marino, M. Boveri, G. Baronetti, M. Laborde, Int. J. Hydrogen Energy 26 (2001) 665.
[3] J. Comas, F. Marino, M. Laborde, N. Amadeo, Chem. Eng. J. 98 (2004) 61.
[4] A.N. Fatsikostas, X.E. Verykios, J. Catal. 225 (2004) 439.
[5] J. Sun, F. Wu, X.-P. Qiu, W.-T. Zhu, Int. J. Hydrogen Energy 30 (2005) 437.
[6] A. Akande, A. Aboudheir, R. Idem, A. Dalai, Int. J. Hydrogen Energy 31 (2006) 1707.
[7] A.P. Ferreira, D. Zanchet, J.C.S. Araújo, J.W.C. Liberatori, E.F. Souza-Aguiar, F.B. Noronha, J.M.C. Bueno, J. Catal. 263 (2009) 335.
[8] L.O.O. Costa, A.M. Silva, L.E.P. Borges, L.V. Mattos, F.B. Noronha, Catal. Today 138 (2008) 147–151.
[9] S.M. de Lima, A.M. Silva, I.O. da Cruz, G. Jacobs, B.H. Davis, L.V. Mattos, F.B. Noronha, Catal. Today 138 (2008) 162.
[10] S.M. de Lima, I.O. da Cruz, G. Jacobs, B.H. Davis, L.V. Mattos, F.B. Noronha, J. Catal. 257 (2008) 356.
[11] S.M. de Lima, A.M. Silva, U.M. Graham, G. Jacobs, B.H. Davis, L.V. Mattos, F.B. Noronha, Appl. Catal. A: Gen. 352 (2009) 95.
[12] P.D. Vaidya, A.E. Rodrigues, Chem. Eng. J. 117 (2006) 39.
[13] P.D. Vaidya, A.E. Rodrigues, Ind. Eng. Chem. Res. 45 (2006) 6618.
[14] P. Ciambelli, V. Palma, A. Ruggiero, Appl. Catal. B: Environ. 96 (2010) 18.
[15] W. Lin, A.A. Herzing, C.J. Kiely, I.E. Wachs, J. Phys. Chem. C 112 (2008) 5942.
[16] C. Li, Y. Song, Y. Chen, Q. Xin, X. Han, W. Li, Stud. Surf. Sci. Catal. 112 (1997) 439.
[17] G. Jacobs, R.A. Keogh, B.H. Davis, J. Catal. 245 (2007) 326.
[18] E. Orücü, F. Gökaliler, A. Erhan Aksoylu, Z. Ilsen Önsan, Catal. Lett. 120 (2008) 198.
[19] L.V. Mattos, F.B. Noronha, J. Catal. 233 (2005) 453.
[20] A. Yee, S.J. Morrison, H. Idriss, J. Catal. 186 (1999) 279.
[21] M.A.S. Baldanza, L.F. de Mello, A. Vannice, F.B. Noronha, M. Schmal, J. Catal. 192 (2000) 64.
[22] E.M. Cordi, J.L. Falconer, J. Catal. 162 (1996) 104.
[23] L.F. de Mello, F.B. Noronha, M. Schmal, J. Catal. 220 (2003) 358.
[24] A. Erdohelyi, J. Raskó, T. Kecskés, M. Tóth, M. Dömök, K. Baán, Catal. Today 116 (2006) 367.
[25] S.M. Stagg-Williams, F.B. Noronha, G. Fendley, D.E. Resasco, J. Catal. 194 (2000) 240.
[26] M.K. Rajumon, R.S. Roberts, F. Wang, P.B. Wells, J. Chem. Soc. Faraday Trans. 94 (1998) 3699.
[27] A.F. Lee, D.E. Gawthrope, N.J. Hart, K. Wilson, Surf. Sci. 548 (2004) 200.
[28] E. Vesselli, G. Coslovich, G. Pomelli, R. Rosei, J. Phys.: Condens. Matter 17 (2004) 6139.